# THE GLUEBALL SPECTRUM FROM LATTICE GAUGE THEORY*

BY C. MICHAEL

D.A.M.T.P., University of Liverpool, Great Britan

*(Received September 1, 1989)*

The glueball spectrum is studied for all $J^{PC}$ values for pure gauge SU(3) colour interactions using lattice gauge theory simulation.

PACS numbers: 11.15.Ha

## *1. Introduction*

The spectrum of pure gauge QCD is of considerable interest. Of course there is also interest in the spectrum of full QCD with dynamical quarks — but experiment already gives the results directly. What is of interest is to understand the way that QCD operates and the pure gauge spectrum is a very valuable waypoint. Since it cannot be determined experimentally, at present the only practical way to determine this spectrum directly from the QCD Lagrangian is by using lattice gauge theory simulation.

This lattice simulation includes the full non-perturbative interaction between gluons but at the expense of introducing a discrete space-time lattice. One of the important cross checks then needed is to vary the spacing of this lattice, and to verify that the results are independent of it. This is referred to as scaling which, if satisfied, allows one to deduce that the results will be valid in the continuum limit. Because lattice regularization, like any regularization scheme for QCD, introduces a dimension or scale, the results appropriate to the continuum limit will be dimensionless ratios such as mass ratios.

In order to understand the current status of glueball results from lattices, I present details of the classification and extraction methods used. This also gives some insight into the colour nature of these states. The main results will follow those of Michael and Teper [1] but I shall also try to review other recent results [2].

---

* Presented at the XXIX Cracow School of Theoretical Physics, Zakopane, Poland, June 2–12, 1989.

## 2. Method

In the continuum, glueball states are classified by their Lorentz covariance properties: momentum $p$, mass $m$, spin $J$, parity $P$, and by their charge conjugation $C$. On a euclidean hypercubic lattice, the relevant symmetries are (*i*) discrete translational invariance if periodic boundary conditions are used (so momentum is conserved but is discrete in steps of $2\pi/L$ for length $L$) and (*ii*) a cubic rotation group $O_h$ with one, two and three-dimensional representations (for non-zero momentum only the space group which is a subgroup of $O_h$ is relevant). These representations have conventional names: the code is that A is one dimensional, E is two dimensional and T is three dimensional. Details are given in elementary texts on group theory in theoretical physics. Since $O_h$ is a subgroup of SU(2), a single SU(2) representation can be decomposed onto one or more $O_h$ represntations. Thus, for example, the $J^P = 2^+$ representation with five magnetic levels is given by degenerate $E^+$ and $T_2^+$ representations with two and three states each. Thus in principle if the spectrum is known accurately for all $O_h$ representations, one can fit them into SU(2) multiplets straightforwardly. Likewise, although full euclidean continuum invariance is not explicit in the lattice calculation, one expects its consequences (such as a relationship between energy and momentum $E^2 = m^2 + p^2$) to be progressively more accurately reproduced as the lattice spacing $a$ is reduced.

The standard use of lattice Monte Carlo simulation is to construct samples of the vacuum on a hypercubic 4-dimensional lattice of size $L^3 \times T$ with periodic boundary conditions. The simplest lattice action is that proposed by Wilson and this is used most commonly. The basic simulation uses a Metropolis or heat-bath algorithm to update the colour state (encoded by an SU(3) matrix) of a link in the presence of all the other links. Repeated application gives sample vacua. Checks are needed that these samples are statistically independent and various methods have been proposed to speed this up (multi-grid methods, over-relaxation, etc.). However, for the results reviewed here, an efficiently vectorized implementation of the basic algorithm on a supercomputer is adequate.

In order to determine the energy of a state in euclidean time, one calculates the average over the sample vacua of a correlation $C(t)$ between quantities at time separation $t$. To study colour singlet states such as glueballs, the correlation of two closed Wilson loops at time separation $t$ is appropriate. For a simple transfer matrix interpretation, it is convenient to take these Wilson loops as purely spatial. Then provided $T$, the length of the lattice in the time direction, is sufficiently large, this correlation $C(t)$ gives information about glueball propagation where the glueball states are created by the loop $P$ acting on the vacuum. Then dependent on the shape, etc. of the loops, one will obtain contributions from glueballs $\alpha$ of energy $E_\alpha$:

$$C(t) = \langle P(0)P(t)\rangle = \sum_\alpha \langle 0|P|\alpha\rangle \exp(-E_\alpha t) \langle \alpha|P|0\rangle.$$

As $t$ is increased, the lightest glueball state will dominate and hence its energy $E$ can be obtained (actually $Ea$, where $a$ is the lattice spacing, is extracted). Now to concentrate on glueballs of specific quantum numbers, one should choose the loop $P$ to have the required rotation, parity and translation symmetries. In practice this means using suitable

TABLE I

The projection table for the cubic rotation group $O$. The object is rotated so that its principal axis is along the top direction and its secondary axis is along the second direction. The third orthogonal direction is included for convenience when taking parity reflections. The numerical coefficients are then given — they need to be normalised.

| | Rotation → | | | | | | | | | | | | | | | | | | | | | | | | | | | |
|---|---|---|---|---|---|---|---|---|---|---|---|---|---|---|---|---|---|---|---|---|---|---|---|---|---|---|---|---|
| R | $x$ | $y$ | $y$ | $-x$ | $-x$ | $-y$ | $-y$ | $x$ | $y$ | $z$ | $z$ | $-y$ | $-y$ | $-z$ | $-z$ | $y$ | $z$ | $x$ | $x$ | $-z$ | $-z$ | $-x$ | $-x$ | $z$ |
| e | $y$ | $x$ | $-x$ | $y$ | $-y$ | $-x$ | $x$ | $-y$ | $z$ | $y$ | $-y$ | $z$ | $-z$ | $-y$ | $y$ | $-z$ | $x$ | $z$ | $-z$ | $x$ | $-x$ | $-z$ | $z$ | $-x$ |
| p | $z$ | $-z$ | $z$ | $-z$ | $z$ | $-z$ | $z$ | $-z$ | $x$ | $-x$ | $x$ | $-x$ | $x$ | $-x$ | $x$ | $-x$ | $y$ | $-y$ | $y$ | $-y$ | $y$ | $-y$ | $y$ | $-y$ |
| ↓ | | | | | | | | | | | | | | | | | | | | | | | | |
| $A_1$ | 1 | 1 | 1 | 1 | 1 | 1 | 1 | 1 | 1 | 1 | 1 | 1 | 1 | 1 | 1 | 1 | 1 | 1 | 1 | 1 | 1 | 1 | 1 | 1 |
| $A_2$ | 1 | −1 | −1 | 1 | 1 | −1 | −1 | 1 | 1 | −1 | −1 | 1 | 1 | −1 | −1 | 1 | 1 | −1 | −1 | 1 | 1 | −1 | −1 | 1 |
| E | 0 | 0 | 0 | 0 | 0 | 0 | 0 | 0 | 1 | 1 | 1 | 1 | 1 | 1 | 1 | 1 | −1 | −1 | −1 | −1 | −1 | −1 | −1 | −1 |
| | 2 | 2 | 2 | 2 | 2 | 2 | 2 | 2 | −1 | −1 | −1 | −1 | −1 | −1 | −1 | −1 | −1 | −1 | −1 | −1 | −1 | −1 | −1 | −1 |
| E | 2 | −2 | −2 | 2 | 2 | −2 | −2 | 2 | −1 | 1 | 1 | −1 | −1 | 1 | 1 | −1 | −1 | 1 | 1 | −1 | −1 | 1 | 1 | −1 |
| | 0 | 0 | 0 | 0 | 0 | 0 | 0 | 0 | −1 | 1 | 1 | −1 | −1 | 1 | 1 | −1 | 1 | −1 | −1 | 1 | 1 | −1 | −1 | 1 |
| | 1 | 0 | 0 | −1 | −1 | 0 | 0 | 1 | 0 | 0 | 0 | 0 | 0 | 0 | 0 | 0 | 0 | 1 | 1 | 0 | 0 | −1 | −1 | 0 |
| $T_1$ | 0 | 1 | 1 | 0 | 0 | −1 | −1 | 0 | 1 | 0 | 0 | −1 | −1 | 0 | 0 | 1 | 0 | 0 | 0 | 0 | 0 | 0 | 0 | 0 |
| | 0 | 0 | 0 | 0 | 0 | 0 | 0 | 0 | 0 | 1 | 1 | 0 | 0 | −1 | −1 | 0 | 1 | 0 | 0 | −1 | −1 | 0 | 0 | 1 |
| | 0 | 1 | −1 | 0 | 0 | −1 | 1 | 0 | 0 | 0 | 0 | 0 | 0 | 0 | 0 | 0 | 1 | 0 | 0 | 1 | −1 | 0 | 0 | −1 |
| $T_1$ | 1 | 0 | 0 | 1 | −1 | 0 | 0 | −1 | 0 | 1 | −1 | 0 | 0 | −1 | 1 | 0 | 0 | 0 | 0 | 0 | 0 | 0 | 0 | 0 |
| | 0 | 0 | 0 | 0 | 0 | 0 | 0 | 0 | 1 | 0 | 0 | 1 | −1 | 0 | 0 | −1 | 0 | 1 | −1 | 0 | 0 | −1 | 1 | 0 |
| | 0 | 0 | 0 | 0 | 0 | 0 | 0 | 0 | 1 | −1 | 1 | −1 | 1 | −1 | 1 | −1 | 0 | 0 | 0 | 0 | 0 | 0 | 0 | 0 |
| $T_1$ | 0 | 0 | 0 | 0 | 0 | 0 | 0 | 0 | 0 | 0 | 0 | 0 | 0 | 0 | 0 | 0 | 1 | −1 | 1 | −1 | 1 | −1 | 1 | −1 |
| | 1 | −1 | 1 | −1 | 1 | −1 | 1 | −1 | 0 | 0 | 0 | 0 | 0 | 0 | 0 | 0 | 0 | 0 | 0 | 0 | 0 | 0 | 0 | 0 |
| | 1 | 1 | −1 | −1 | 1 | 1 | −1 | −1 | 0 | 0 | 0 | 0 | 0 | 0 | 0 | 0 | 0 | 0 | 0 | 0 | 0 | 0 | 0 | 0 |
| $T_2$ | 0 | 0 | 0 | 0 | 0 | 0 | 0 | 0 | 1 | 1 | −1 | −1 | 1 | 1 | −1 | −1 | 0 | 0 | 0 | 0 | 0 | 0 | 0 | 0 |
| | 0 | 0 | 0 | 0 | 0 | 0 | 0 | 0 | 0 | 0 | 0 | 0 | 0 | 0 | 0 | 0 | 1 | 1 | −1 | −1 | 1 | 1 | −1 | −1 |
| | 0 | 0 | 0 | 0 | 0 | 0 | 0 | 0 | 0 | −1 | −1 | 0 | 0 | 1 | 1 | 0 | 1 | 0 | 0 | −1 | −1 | 0 | 0 | 1 |
| $T_2$ | 1 | 0 | 0 | −1 | −1 | 0 | 0 | 1 | 0 | 0 | 0 | 0 | 0 | 0 | 0 | 0 | 0 | −1 | −1 | 0 | 0 | 1 | 1 | 0 |
| | 0 | −1 | −1 | 0 | 0 | 1 | 1 | 0 | 1 | 0 | 0 | −1 | −1 | 0 | 0 | 1 | 0 | 0 | 0 | 0 | 0 | 0 | 0 | 0 |
| | 0 | 0 | 0 | 0 | 0 | 0 | 0 | 0 | 1 | 0 | 0 | 1 | −1 | 0 | 0 | −1 | 0 | −1 | 1 | 0 | 0 | 1 | −1 | 0 |
| $T_2$ | 0 | −1 | 1 | 0 | 0 | 1 | −1 | 0 | 0 | 0 | 0 | 0 | 0 | 0 | 0 | 0 | 1 | 0 | 0 | 1 | −1 | 0 | 0 | −1 |
| | 1 | 0 | 0 | 1 | −1 | 0 | 0 | −1 | 0 | −1 | 1 | 0 | 0 | 1 | −1 | 0 | 0 | 0 | 0 | 0 | 0 | 0 | 0 | 0 |

linear combinations of translated and rotated loops. The sum over translations $\sum \exp(2\pi i \boldsymbol{n}\boldsymbol{x}/L)P(\boldsymbol{x})$ yields momentum $\boldsymbol{p} = 2\pi \boldsymbol{n}/La$ where $(n_1, n_2, n_3)$ are integers and the spatial size is $L^3$. Most results come from the zero momentum combination, but useful information is also obtainable from small non-zero momentum values. For zero momentum, the relevant sum over rotations $R$ of the loop $P$ is given by the projection table PJ (rep, $R$) for $O$:

$$\sum_R \mathrm{PJ}\,(\mathrm{rep}, R)R(P).$$

For convenience this projection table for $O$ is given in Table I. A sum or difference of parity reflections then yields parity eigenstates, and taking real or imaginary parts of the loop gives $C$ even or odd.

Even when a loop combination $P$ has been constructed which has a unique momentum, space group representation, parity and charge conjugation, it is important to optimize the overlap of $P$ with the lowest glueball. Thus $P$ acting on the vacuum can be expanded in a glueball basis (including two particle continuum states as well):

$$P|0\rangle = \sum_\alpha c_\alpha |\alpha\rangle.$$

The observed correlation $C(t)$ is then given by

$$C(t) = \sum_\alpha |c_\alpha|^2 \exp(-E_\alpha t)$$

from which the lowest glueball energy can be extracted by

$$E_1 = \lim_{t\to\infty} m_{\text{eff}}(t) \quad \text{where} \quad a m_{\text{eff}}(t) = -\log(C(t+a)/C(t)).$$

Since $C(t)$ decreases with increasing $t$ while the error stays relatively constant, the values of $C$ for small $t$ have smallest relative errors. Thus $m_{\text{eff}}$ is best determined at small $t$. The relative effect of excited glueballs is least at large $t$, however, so the systematic errors in extracting $E_1$ are least where the statistical errors are largest. Thus it is important to optimise the overlap of the ground state $|1\rangle$, nemely

$$|c_1|^2 = |\langle 0|P|1\rangle|^2 = \exp\{-\sum_{t=0}^{\infty} a(m_{\text{eff}}(t) - E_1)\}$$

in order to reduce the error in the determination of $E_1$ (here we normalise $\sum_\alpha |c_\alpha|^2 = 1$). There are several ways to improve the determination of $E_1$: (*i*) by measuring simultaneously correlations between several different shaped loops $P(j)$ and using a variational method to find the optimum combination of them to enhance the ground state contribution, (*ii*) to construct loops $P$ which have a very large overlap by using a smearing or fuzzing procedure. Both of these help, but the recent major improvement in glueball mass determinations has come predominantly from the judicious use of fuzzing. The variational method, however, has especial value in enabling further excited states in the spectrum to be studied. In principle an $N$ loop basis with an $N \times N$ matrix of correlations measured enables $N$ energy levels to be extracted.

After much experimentation, an efficient fuzzing algorithm has been found to be [3]

$$U \Rightarrow P[U(x,\mu)U(x+\mu,\mu) + \sum_{\nu\neq\mu,\,\nu\neq 0} U(x,\nu)U(x+\nu,\mu)U(x+\nu+\mu,\mu)U^\dagger(x+2\mu,\nu)],$$

where the sum is over 4 staples in spatial directions orthogonal to $\mu$, $P$ implies a projection back to the nearest element of SU(3) and the notation is that $U(x,\mu)$ is the colour matrix corresponding to the link from position $x$ in direction $\mu$. See Fig. 1. The new fuzzed link is of twice the length of the original links. This prescription can then be iterated to give

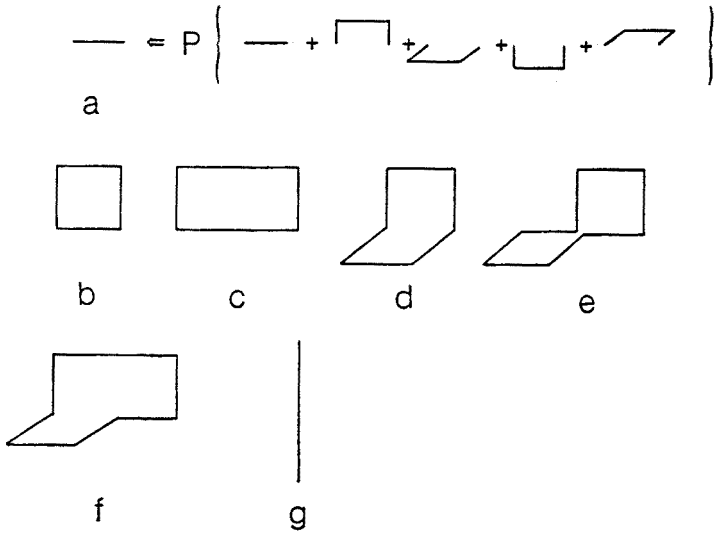


Fig. 1. (a) The fuzzing prescription. The $P$ symbol indicates a projection to the nearest element of SU(3). (b–f) Closed paths used as glueball operators. (g) A path encircling the periodic boundary conditions used as a torelon operator

superlinks of length 2, 4, 8, etc. The motivation for such a prescription is that it averages over the colour fields in a given space-time region in a rather smooth way and thus is less sensitive to the ultraviolet fluctuations present in the lattice vacuum samples. This then reproduces the ground state well since the ground state has the smoothest colour fields. Another motivation is that the ground state of colour flux between static colour sources is also known to be rather delocalized and to spread into a transverse region comparable with the length. The upshot is that low energy glueballs are very efficiently made from such fuzzed links. For instance 90% overlaps are obtainable — which gives very accurate mass determinations.

With the same loop combination at time 0 and $t$, the effective masses extracted from the correlation are upper limits (i.e. $m_{\text{eff}}(t) > E_1$) and monotonically decrease as $t$ increases. To estimate the value of $E_1$ itself, a typical algorithm is to find the least value of $t$ where $m_{\text{eff}}(t)$ and $m_{\text{eff}}(t+a)$ agree within their statistical errors and to use the smaller of these two values of $m_{\text{eff}}$ with the errors from the $t+a$ value. This algorithm is conservative in that the error comes from $t+a$ which is normally larger than that from $t$. This serves to take account of the systematic error in the extrapolation in $t$.

As well as glueball observables obtained by measuring correlations of spatial Wilson loops at time separation $t$, one can consider spatial Polyakov lines which encircle the periodic spatial boundary — see Fig. 1. For an SU($N$) pure gauge theory, invariance under the centre group Z($N$) means that there are different sectors labelled by an integer mod ($N$) in each space direction. The simplest such sector has integers 1, 0, 0 and corresponds to one unit of electric flux in the $x$-direction. The states of this sector are orthogonal to glueball states (integer 0, 0, 0) and are called torelons. The torelon sector also has further symmetry

classification: momentum transverse to the electric flux direction and representations of $D_{4h}$ to account for rotations, reflections etc. The most symmetric state is isotropic under $D_{4h}$ and has zero momentum and this is the most commonly studied state. This torelon can be thought of as a colour flux line encircling the boundary and so it has energy $K_{\text{eff}}L$ where $K_{\text{eff}}$ is an effective string tension. This string (colour flux line) has no end effects compared to that between static colour sources and so the string tensions defined in these two different ways may not be identical for finite separations. Again it turns out that a fuzzing prescription enhances the torelon overlap. Thus accurate string tension values can be obtained on spatial lattices as large as $20^3$.

### 3. *Results*

The best determined energy levels are those corresponding to the torelon and the $0^{++}$ and $2^{++}$ glueball masses. Interpreting the measured torelon mass $Ea$ in lattice units as $K_{\text{eff}}(L/a)a^2$, one can see whether the lattice spacing $a$ has the dependence on the bare coupling constant (where $\beta = 6/g^2$ is quoted conventionally in lattice evaluations with SU(3) colour) that follows from perturbative QCD. This corresponds to a behaviour

$$\frac{Ea}{\Lambda_L a} = Ea\left(\frac{8\pi^2}{33}\beta\right)^{-\frac{51}{121}} e^{\frac{4\pi^2}{33}\beta}$$

where $\Lambda_L$ is the lattice regularization scale. Thus $\sqrt{K_{\text{eff}}}/\Lambda_L$ should be constant as $\beta$ increases ($g$ decreases) if perturbation theory is applicable. For SU(3) pure gauge one obtains values [1] of 94. 1(1.2), 89.4(0.9) and 82.0(1.6) at $\beta$ values of 5.9, 6.0 and 6.2 respectively. Thus we see a statistically significant deviation from asymptotic scaling. This is in accord with results from Monte-Carlo Renormalization Group studies. These results are equivalent to an effective $\beta$-function which is 70% of the two loop perturbative value. This is not a great surprise since the bare coupling constant has a value of $g \approx 1$ and thus low order perturbation theory need not be very precise. Evaluations at significantly higher values of $\beta$ will be needed to investigate the approach to asymptotic scaling.

Rather than use perturbation theory to determine the dependence $a(g)$, one can just determine dimensionless ratios and check the weaker assumption (called scaling) that the dependence $a(g)$ is universal and so cancels. The best determined such ratio is $m(0^{++})/\sqrt{K_{\text{eff}}}$ and this is illustrated in Fig. 2. At sufficiently large $\beta$, it is consistent with scaling. However, this ratio at lower $\beta$ is much less. This is the root of the increase in recent years of the $0^{++}$ glueball mass: $\sqrt{K_{\text{eff}}} = 0.44$ GeV is used to set the scale (from the slope of Regge trajectories) and hence $m(0^{++})$ has increased since its ratio to $\sqrt{K_{\text{eff}}}$ has increased with $\beta$ (and hence with time since larger $\beta$ corresponds to smalller lattice spacing $a$ and has become accessible to computer investigation more recently since larger computing resources are needed). Fig. 2 illustrates the remaining uncertainty in determining the glueball masses in physical units: a further increase of the ratio with increasing $\beta$ is not ruled out. As well as that possibility, it must also be kept in mind that the value of $K_{\text{eff}}$ taken from experiment includes dynamical quark effects. These might easily cause a 20%

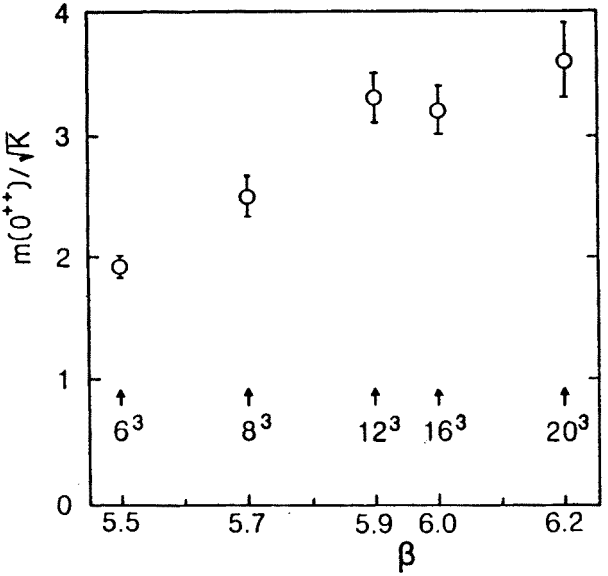


Fig. 2. The ratio of the $0^{++}$ glueball mass to $\sqrt{K_{\text{eff}}}$ where the effective string tension $K_{\text{eff}}$ is obtained from the energy of a flux line encircling the periodic spatial boundary. Results from Refs [1, 4] are at $\beta$-values shown and with spatial volumes as shown

change in the value of $K_{\text{eff}}$ when removed. This estimate of 20% comes from the perturbative change in the $\beta$-function which is one of the few cases where dynamical quark effects are accurately known. Predictions for mass ratios between glueballs do not depend on these uncertainties in the energy scale and may be taken more seriously as predictions for experiment.

In order to be sure that lattice results are not affected by the boundary used, it is necessary to vary the spatial size at fixed lattice spacing $a$. The large volume results should be independent of the volume and this is indeed found. For sizes less than $9m(0^{++})^{-1}$, large deviations are found — especially for the $2^{++}$ glueball which splits into a lighter $E^{++}$ component and a heavier $T_2^{++}$ component. A convenient measure of the spatial size is to define $z(\text{rep}) = m(\text{rep})L$ for an $L^3$ spatial volume. Thus $z(0^{++}) > 9$ is found to be the large volume region. Analytic calculations [2] are possible up to $z \approx 4$ by integrating out the non-zero momentum modes and solving numerically the resulting effective Lagrangian in the zero-momentum modes taking care also of the topological structure of the vacuum. Unfortunately the large volume results from full lattice calculations do not overlap this region where the zero-mode approximation applies.

A summary of the low lying glueball states determined by Michael and Teper [1] is given in table II. The agreement between different lattice $\beta$-values and sizes $L$ is good as is the agreement between $E^{++}$ and $T_2^{++}$ masses (making $2^{++}$) and between $E^{-+}$ and $T_2^{-+}$ masses (making $2^{-+}$). The first excited $A_1^{++}$ $(0^{++})$ state is also determined. Other groups [2] have obtained results for the lowest $A_1^{++}$ state and these agree well. The $2^{++}$ state was claimed to lie lower in some earlier work but the consensus [2] is now that the $2^{++}/0^{++}$

TABLE II

Glueball mass ratios to $\sqrt{K_{\text{eff}}}$

| $\beta$ | 5.9 | 6.0 | 6.0 | 6.0 | 6.2 | Ave. Large |
|---|---|---|---|---|---|---|
| $L$ | 12 | 10 | 16 | 20 | 20 | Vol. |
| $A_1^{++}$ | 3.3(2) | 3.8(2) | 3.2(2) | 3.4(5) | 3.6(3) | 3.5(2) |
| $A_1^{++\prime}$ | | 5.5(3) | 6.1(11) | 6.0(12) | 6.5(5) | 6.3(4) |
| $E^{++}$ | 5.6(5) | 5.1(3) | 5.1(3) | 5.1(6) | 5.6(3) | 5.3(2) |
| $T_2^{++}$ | | 6.5(6) | | | 5.4(3) | |
| $A_1^{-+}$ | 4.3(21) | 6.4(7) | 5.6(6) | 7.1(23) | 7.1(11) | 6.3(7) |
| $E^{-+}$ | | 8.4(3) | 5.8(8) | | 7.0(9) | 6.6(10) |
| $T_2^{-+}$ | | 8.5(3) | | | 7.4(7) | |
| $T_1^{+-}$ | 8.5(28) | 8.0(12) | 6.7(10) | 5.9(21) | 6.9(5) | 6.9(5) |

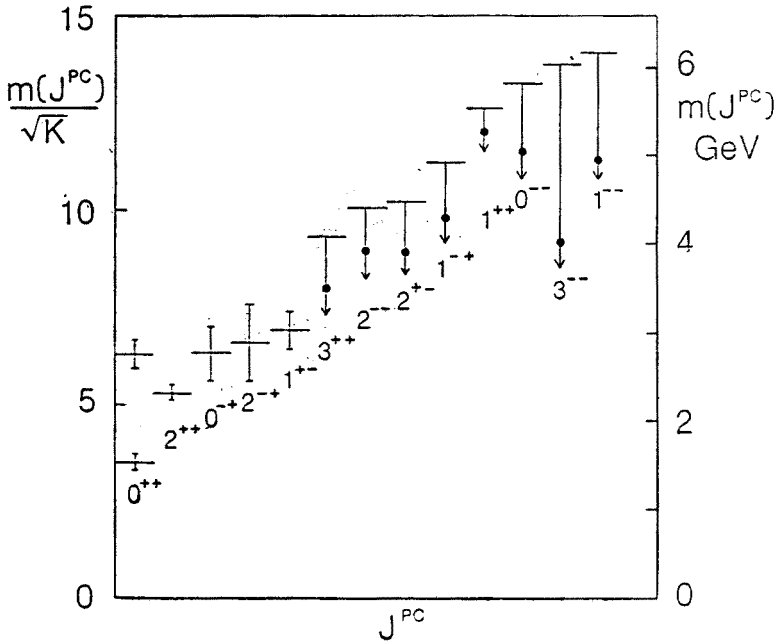


Fig. 3. Glueball masses in units of $\sqrt{K_{\text{eff}}}$ from Michael and Teper [1]. The values are from Table II and the upper limits are $2\sigma$ with 2 : 1 $t$-ratio effective masses. For the $0^{+-}$, $3^{+-}$ and $3^{-+}$ states there are only very high upper limits. Setting the energy scale by using $\sqrt{K} = 0.44$ GeV gives the right hand scale — there is an inherent systematic error in this scale since $K$ is determined experimentally with dynamical quarks rather than pure gauge

mass ratio is around 1.5. The other $J^{PC}$ states have not been accessible in most other work. The low-lying glueball states determined by the lattice calculations have $J^{PC}$ values which are broadly consistent with those expected from phenomenological models.

For all remaining $J^{PC}$ states, the lattice determination gives upper limits — they are illustrated in Fig. 3. Since the 2/1 and 3/2 $t$-ratio variational results of Michael and Teper agree well when they are both measurable (this is the source of the mass determinations quoted above), one can use the 2/1 $t$-ratio results for all cases as a guide to the asymptotic

mass value even when there is no cross check coming from the 3/2 $t$-ratio because the statistical error is too large. In this spirit, they investigate the oddball states. These are the $J^{PC}$ values not allowed for $q\bar{q}$ mesons: $0^{--}$, $0^{+-}$, $1^{-+}$. $2^{+-}$, etc. Since $O_h$ representations correspond to a sequence of $J$-values, one cannot distinguish oddball states from high-$J$ non-exotic states in most cases. Thus the $A_1^{--}$, $A_1^{+-}$, $A_2^{-+}$, $E^{+-}$, $T_1^{-+}$, and $T_2^{+-}$ representations can have non-exotic $4^{--}$, $9^{+-}$, $6^{-+}$, $5^{+-}$, $4^{-+}$ and $3^{+-}$ contributions as well as the spin-exotic $0^{--}$, $0^{+-}$, $3^{-+}$, $2^{+-}$, $1^{-+}$ and $2^{+-}$ contributions. Nevertheless, there is no evidence for *any* such low lying states from the 2/1 $t$-ratio effective masses. Indeed the lowest such mass is for the $T_2^{+-}$ which is a relatively poor oddball signal since it gets non-exotic $3^{+-}$ contributions. Thus there is no evidence for the presence of oddball states at masses lower than twice the ground state $0^{++}$ mass. This conclusion is at variance with earlier work [5] which claimed evidence for a $1^{-+}$ oddball state at a mass similar to the $2^{++}$ state. That work was based on a much less thorough study than more recent work.

## 4. Conclusions

The main technical advance which has been responsible for the recent improvements in glueball mass determination has been the use of fuzzy glueball operators which have, for example, a 90% overlap to the ground state $0^{++}$ glueball at $\beta = 6.2$. Another powerful feature is that the variational method with many path shapes allows a probe of all $J^{PC}$ values. Thus one can now determine the low-lying glueball mass spectrum for a range of $\beta$ values and lattice sizes $L$. This enables a check of finite size effects and of scaling. The conclusions are that for $\beta > 5.8$ and $m(A_1^{++})L > 9$, one obtains consistent results — which can then be identified with the continuum limit of pure gauge QCD. The spectrum is illustrated in Fig. 3.

Since one can model the low lying glueballs accurately by using combinations of fuzzy paths acting on the vacuum, one can study more detailed glueball properties. Exploratory studies of glueball sizes and of glueball decay matrix elements have already been made [6, 7] using lattice gauge theory simulation.

## REFERENCES


[1] C. Michael, M. Teper, *Nucl. Phys.* **B314**, 347 (1989).

[2] P. Van Baal, A. S. Kronfeld, *Nucl. Phys.* **B**, Proc. Suppl., to be published; preprint CERN TH 5241/88, Fermilab CONF-88/183-T.

[3] M. Teper, *Phys. Lett.* **183B**, 345 (1986); **185B**, 121 (1987).

[4] P. de Forcrand et al., *Phys. Lett.* **160B**, 137 (1985); **152B**, 107 (1985).

[5] K. Ishikawa et al., *Phys. Lett.* **120B**, 387 (1983).

[6] G. A. Tickle, C. Michael, Liverpool preprint LTH 235.

[7] C. Michael, Liverpool preprint LTH 229, *Nucl. Phys.* **B**, to be published.